PHYSICAL REVIEW B VOLUME 48, NUMBER 20 15 NOVEMBER 1993-II

Application of gradient corrections to density-functional theory for atoms and solids

Yu-Min Juan and Efthimios Kaxiras
Department of Physics and Division of Applied Sciences, Harvard University, Cambridge, Massachusetts 02138

(Received 29 October 1992; revised manuscript received 25 February 1993)

Gradient corrections have been shown to improve the accuracy of density-functional theory (DFT) when applied to homonuclear dimers, small molecules, and bulk properties of transition metals (such as Fe). A more thorough evaluation is needed before adopting these corrections for large-scale computations in solids. We investigate a broad range of different systems by using the most recently proposed gradient correction to DFT by Perdew and Wang, which is expected to give a marked improvement over earlier attempts. We find that when this correction is used to calculate the energy of atoms it gives better agreement with experiment than the local-density approximation (LDA). When applied to bulk properties, this correction gives results which are not consistently better and tend to overcorrect LDA results.

I. INTRODUCTION

Density-functional theory[1] (DFT) has proved to be a versatile and valuable tool in modern computational physics. The local density approximation[2] (LDA) is the most widely used implementation of DFT, which renders applications to a variety of problems computationally feasible.[3] However, even with its well recognized success, LDA has several limitations (see, e.g., Ref. 3). Accordingly, improvements to LDA have been sought for many years. Ortiz and Ballone[4] recently pointed out that gradient corrections constitute a promising approach from both a computational and a conceptual point of view. In their calculation for homonuclear dimers, such corrections gave an improvement over LDA results in every respect. It was also reported by Bagno, Jepsen, and Gunnarsson[5] that by applying gradient corrections, the solid properties of third row elements are predicted more accurately. Despite these encouraging indications, a more thorough test for finite systems (atoms, molecules, clusters) as well as infinite systems (crystalline solids) is necessary before adopting these corrections for large-scale computations. Recently some tests of this type have been reported by Perdew *et al.*,[6] Ortiz,[7] García *et al.*,[8] and Körling and Häglund.[9]

In this work, we present a test of gradient corrections to DFT for a broad range of atoms and solids. In the present calculation we used the gradient-corrected exchange-correlation functional that was recently introduced by Perdew[10,11] in its spin-unpolarized form (it will be referred to as PW91). For the convenience of the reader we reproduce the PW91 functional in Appendix A. This newly proposed functional is expected to give marked improvements over earlier attempts. The reasons for this expectation are (1) The PW91 functional was constructed by analyzing the behavior of exchange and correlation under conditions for which exact results can be obtained, rather than by fitting computational results; specifically, it satisfies the proper sum rules and scaling relations for exchange and correlation. (2) Unlike other schemes, this functional treats exchange and correlation effects on an equal footing, which is more consistent from a first-principles theoretical point of view. (3) An earlier version of this approach[11] appeared to give improved agreement with experiment for bulk properties of transition metals, such as Fe.[5] We find that PW91 improves the calculation of atomic energies over LDA results. However, when applied to bulk properties of solids PW91 does not give a consistent improvement over LDA results.

The remainder of this paper discusses the application of PW91 to atoms (Sec. II), and to several types of solids, including metals, semiconductors, and insulators (Sec. III). We conclude in Sec. IV with comparison to other calculations and some remarks on the usefulness of this gradient correction.

II. APPLICATION TO ATOMS

We first consider the application of the PW91 gradient correction to scalar non-relativistic all-electron calculations for atoms. The elements we considered range from alkali metals to inert gases. Specifically, they include the second, third, and fourth rows of the Periodic Table, except for the transition metals, for which some results have already been reported in the literature.[4] The results of these calculations, which employed the standard logarithmic grid for the radial variable,[12] are given in Table I. The total energy, exchange energy, and correlation energy are compared to experimental measurements where available and to LDA results. By using the PW91 functional, one obtains a lower total energy and exchange energy but a higher correlation energy, all in better agreement with experiment than LDA results. A noticeable point is that for heavier elements, the agreement between calculation and experiment seems to worsen (although still better than LDA, where comparison to experiment is possible). The reason is most likely due to the neglect of relativis-

TABLE I. Atomic total energy, exchange energy, and correlation energy calculated from LDA and PW91. Experimental data for the total energy are from Ref. 13. Experimental data for exchange and correlation energy are from Ref. 14, except for Ar; the correlation energy for Ar is from Ref. 15. All values are in atomic units.

	X		
	$-E_{tot}$	$-E_x$	$-E_c$
LDA calculation			
PW(91) calculation			
Experiment			

Li			**Be**			**B**			**C**			**N**			**O**			**F**			**Ne**		
7.334	1.651	0.161	14.446	2.514	0.226	24.343	3.522	0.297	37.424	4.727	0.376	54.023	6.137	0.461	74.469	7.764	0.552	99.094	9.617	0.648	128.227	11.703	0.749
7.480	1.782	0.058	14.673	2.724	0.087	24.656	3.812	0.119	37.828	5.101	0.158	54.524	6.601	0.201	75.072	8.324	0.249	99.804	10.278	0.300	129.049	12.472	0.354
7.479	1.781	0.045	14.667	2.67	0.094	24.654		0.125	37.844		0.156	54.587		0.189	75.063			99.725			128.928	12.110	0.387
Na			**Mg**			**Al**			**Si**			**P**			**S**			**Cl**			**Ar**		
161.433	13.516	0.819	199.133	15.448	0.900	241.309	19.547	0.980	288.192	19.547	1.067	339.940	21.778	1.158	396.710	24.134	1.253	458.657	26.618	1.350	525.938	29.233	1.450
162.379	14.413	0.382	200.198	16.463	0.419	242.498	20.804	0.458	289.506	20.804	0.504	341.382	23.161	0.554	398.282	25.646	0.608	460.364	28.263	0.664	527.782	31.015	0.723
162.245			200.043		0.426	242.336			289.348			341.240			398.100			460.149			527.549	30.18	0.731
K			**Ca**			**Ga**			**Ge**			**As**			**Se**			**Br**			**Kr**		
598.192	31.640	1.525	675.733	34.133	1.608	1921.831	71.903	2.818	2073.792	75.729	2.922	2232.520	79.627	3.029	2398.097	83.602	3.137	2570.605	87.659	3.247	2750.132	91.802	3.359
600.178	33.568	0.755	677.855	36.192	0.796	1925.508	75.484	1.487	2077.618	79.458	1.546	2236.498	83.503	1.608	2402.227	87.628	1.673	2574.890	91.838	1.739	2754.573	96.135	1.807
																						93.900	

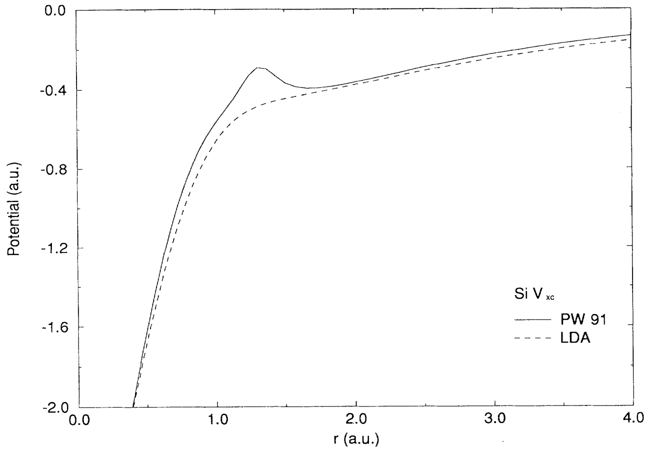

FIG. 1. The all-electron exchange-correlation potential for the Si atom as given by the LDA and PW91 functionals. The shoulder region at $r \simeq 1.3$ a.u. is due to sharp variations in the density.

tic effects which become more important for the heavier atoms. PW91 appears to overcorrect the LDA results in some cases, even though the difference with experiment is small. For example, the total energy of a Si atom is -288.192 from LDA and -289.506 from PW91, while the experimental result is -289.348 (all numbers are in units of 1 hartree equals 27.2116 eV).

For a more detailed look at the effect of PW91 on the atomic calculations, we present an example in Fig. 1. In this figure, we display the exchange-correlation potential for Si as obtained by LDA and PW91. In general, LDA gives a more negative exchange-correlation potential than PW91. Except for the shoulder region, where the large difference is due to the gradient correction term which arises from a rapid change in the density, the difference between LDA and PW91 is actually quite small. Nevertheless, this small difference in the exchange-correlation potential gives significant differences in the energies (see Table I).

III. APPLICATION TO SOLIDS

In order to perform consistent first-principles pseudopotential calculations for solids, it is necessary to construct new pseudopotentials. The reasons are both conceptual and practical. Pseudopotentials that are available in the literature, such as the ones by Bachelet, Hamann, and Schlüter[16] (BHS) were constructed from LDA all-electron calculations. If these potentials were to be used in the PW91 solid calculations, then the screening effect for core electrons would be approximated by LDA while the screening effect for valence electrons will be approximated by the PW91 functional, which evidently is not a self-consistent approach. Moreover, it was found by Ortiz and Ballone[4] that a self-consistent pseudopotential that incorporates gradient corrections gives different results from a BHS pseudopotential. The details of the construction of the pseudopotentials used in the present calculation are given in Appendix B.

We performed total energy pseudopotential calculations for two simple metals (Na and Mg), one *sp*-bonded metal (Al), two elemental semiconductors (Si and Ge), one compound semiconductor (GaAs), and one inert gas crystal (Ar). The calculations were done by using a plane-wave basis. For the LDA calculations, we used the exchange-correlation potential of Ceperley and Alder as parametrized by Perdew and Zunger.[15] The use of a plane-wave basis is advantageous in that the gradient and the Laplacian of the density needed in PW91 can be obtained easily by fast Fourier transforms (FFT's). In the PW91 calculation only nine additional FFT's are needed, which results in a very modest increase of computational time (less than 3%).

The ground state properties of each solid were obtained by minimizing the energy with respect to the lattice constant. In our present calculation, we fitted the results to the Murnaghan equation of state,[17] which then gives the equilibrium lattice constant and bulk modulus. In order to obtain a reliable cohesive energy one needs to calculate the energy of the solid with the same degree of accuracy as that of the isolated atom. The latter is obtained by integration of the Schrödinger equation and is essentially exact (within the limits of DFT). The energy of the solid converges variationally with the size of the plane-wave basis. For this reason, we first calculate the ground state energy corresponding to the calculated equilibrium lattice constant for several values of the cutoff energy E_c, which is the highest plane-wave kinetic energy and determines the size of the basis. The cutoff energy ranges from 12 to 20 Ry, except for Ar, in which case E_c ranges from 16 to 32 Ry. Then, we fitted the calculated total energies to $E = E_0 + \lambda / E_c^\gamma$ in order to obtain the asymptotic value of the total energy E_0 (λ and γ are fitting parameters; the optimal value of γ is 2.5). We find that the error introduced by using this formula is less than 0.1% (this was estimated by comparing the fitted result to the calculated result for the highest cutoff energy). In order to include spin-polarization effects, we used the empirical formula $\Delta E_p = -0.18 \times n_p^2$ eV ($n_p = n_\uparrow - n_\downarrow$, $n_\uparrow$ being the number of electrons with spin up and $n_\downarrow$ the number of electrons with spin down) to estimate the shift in the total energy of the pseudoatoms in spin-polarized configurations. Spin-polarized calculations for nonmagnetic solids are expected to have negligible effect on the total energy E_0. The cohesive energy is then determined by the difference between E_0 and the total atomic energy calculated for the pseudoatom.

The total energy vs lattice constant curves from LDA and PW91 for Na, Mg, and Al are shown in Fig. 2(a) and for Si, Ge, GaAs, and Ar in Fig. 2(b). The curves from the PW91 calculations are flatter and they are shifted to the right compared to the LDA curves. Thus the PW91 functional gives a larger lattice constant and smaller bulk modulus than LDA. The latter approximation overestimates the cohesive energy in most cases, and gives too small lattice constants compared to experiment. The results for the calculations of ground state properties of solids are summarized in Table II. Except for the simple metals Na and Mg, the results from PW91 seem to overcorrect the LDA results. Specifically, the PW91 results give a lattice constant which is bigger than experiment by a significant amount. For example, the PW91 results give lattice constants which are higher than experiment by 3%, 5%, and 5% for Si, Ge, and GaAs, respectively, whereas LDA results give lattice constants which are smaller than experiment by 1%, 2%, and 2% for the same solids. For the bulk modulus, the results from the PW91 calculations are better for Na, Mg, Al, and Ar, since the LDA values are too high for these three elements. But for Si, Ge, and GaAs, the bulk moduli from the PW91 calculations are worse than the LDA results, which were already underestimates of the experimental values. For the cohesive energy, the PW91 calculations give an improvement over the LDA results in most cases, even though the PW91 cohesive energies are still larger (in absolute value) than experiment. For Ar, we note that the energy vs volume curve is much flatter than other solids, making the prediction of the equilibrium lattice constant and bulk modulus more difficult. In summary, we find that use of the PW91 functional gives a weaker binding between atoms in a solid, resulting in larger lattice constants and smaller bulk moduli. The deviation from experiment depends somewhat on the character of the solid, but in many cases it is larger than the deviation of LDA results from experiment.

The calculated band gaps for the semiconductors and

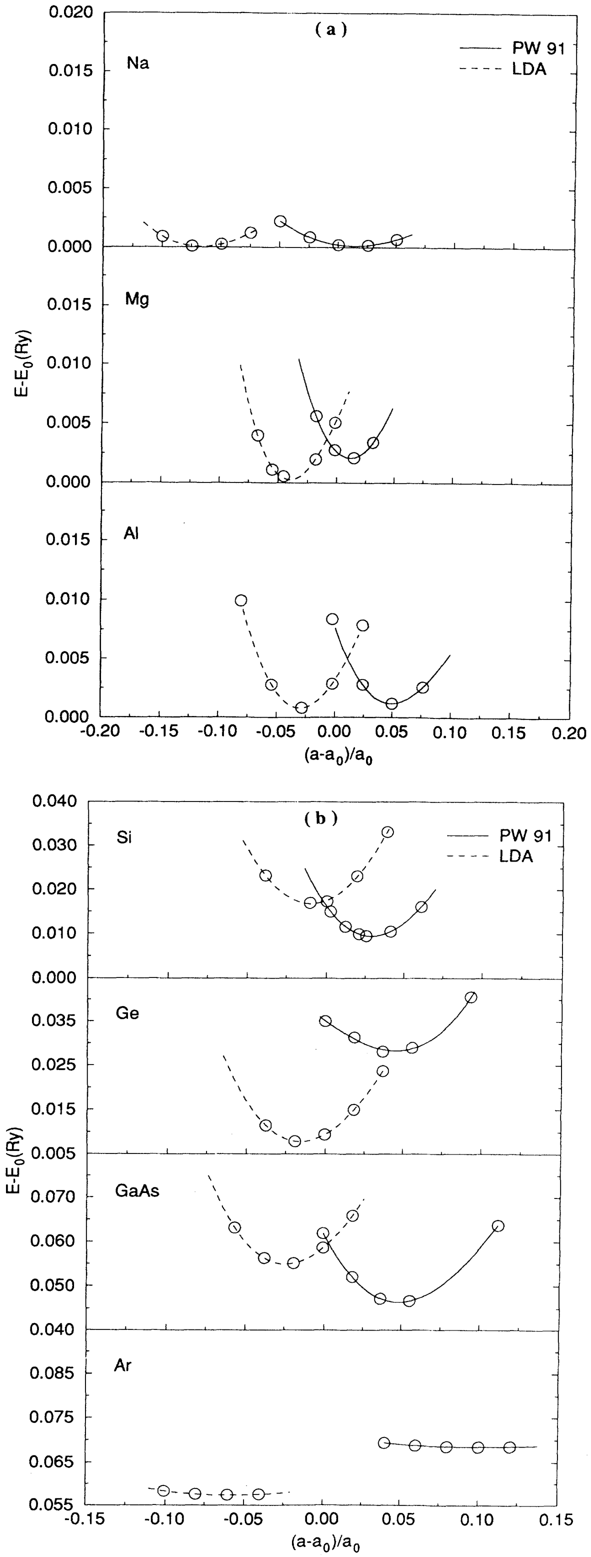

FIG. 2. (a) Comparison of total energy vs lattice constant curves for Na, Mg, and Al as given by the LDA and PW91 functionals. The dots are calculated values, the lines are fits to Murnaghan's equation of state. a_0 is the experimental lattice constant, E_0 is the asymptotic value of the solid's total energy (see text). (b) Same as in (a), for Si, Ge, GaAs, and Ar.

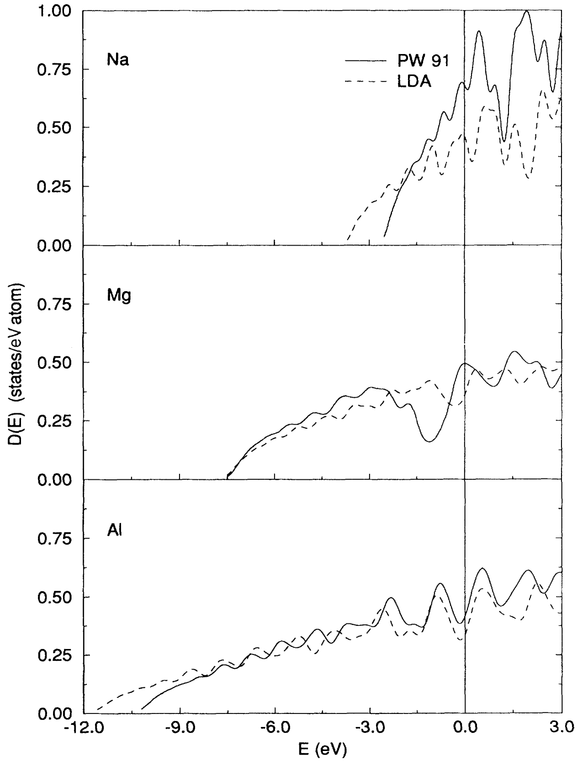

FIG. 3. Density of states (including spin degeneracy) for Na, Mg, and Al calculated from LDA and PW91. The Fermi energy is taken to be zero.

TABLE II. Lattice constant, bulk modulus, and cohesive energy calculated from LDA and PW91. The experimental data for lattice constants are taken from Ref. 18, except for GaAs, which is from Ref. 19. The experimental data for bulk modulus and cohesive energy are from Ref. 20, except for GaAs, which are from Refs. 21 and 22. The unit for lattice constant is Å; the unit for bulk modulus is 10^{10}dyn/cm^2; the unit for cohesive energy is eV.

	X		
	lattice constant	**bulk modulus**	**cohesive energy**
LDA calculation			
PW(91) calculation			
Experiment			

Na			**Mg**			**Al**			**Si**			**Ge**			**GaAs**			**Ar**		
3.74	10.65	1.51	3.08	41.77	2.00	3.93	87.65	4.14	5.38	96.57	5.38	5.57	74.72	4.53	5.51	77.09	8.58	4.94	6.46	0.419
4.29	5.68	1.18	3.25	37.70	2.06	4.25	61.07	3.22	5.59	85.22	4.64	5.92	58.12	3.71	5.92	54.59	6.43	5.83	2.75	0.066
4.23	6.80	1.11	3.21	35.40	1.51	4.05	72.20	3.39	5.43	98.80	4.63	5.66	77.20	3.85	5.65	75.57	6.52	5.26	1.60	0.080

the insulator we have considered, at both the theoretically predicted equilibrium lattice constant and the experimentally measured one, are given in Table III. At the experimentally measured lattice constant, PW91 gives consistently a better band gap than LDA. At the theoretically predicted lattice constant, however, it cannot be said conclusively whether PW91 is better or worse than LDA in predicting band gaps. This is to be expected since the band gap depends on the lattice constant, and PW91 and LDA give significantly different equilibrium lattice constants. In Fig. 3 we compare the density of states for the three metals we have considered, calculated from LDA and PW91. As can be seen from this figure, the PW91 calculation gives a narrower bandwidth and a larger density of states at the Fermi level. This is because PW91 gives a "softer" solid than LDA, and the bandwidth scales with the strength of the interaction between atoms.

TABLE III. Band gap calculated from LDA and PW91. $a_0^{\rm th}$ is the equilibrium lattice constant predicted by theory. $a_0^{\rm expt}$ is the equilibrium lattice constant measured from experiment. The experimental data are taken from Ref. 23, except for Ar, which is from Ref. 24. The unit is eV.

	X	
	at a_0^{th}	at a_0^{exp}
LDA calculation		
PW(91) calculation		
Experiment		

Si		Ge		GaAs		Ar	
0.49	0.54	0.30	0.02	1.03	0.58	8.41	8.33
0.81	0.69	0.05	0.61	0.62	1.43	8.25	8.45
	1.17		0.79		1.52		14.30

For a more detailed look at the effect of gradient corrections, we show in Fig. 4(a) the difference between the PW91 and LDA exchange correlation energy functionals for Si. Figure 4(b) presents a comparison between PW91 and LDA exchange-correlation potentials, which are essentially the functional derivatives of the energy with respect to density. In both cases the most important difference between LDA and PW91 occurs near the atomic nuclei. This is not surprising, since the density varies significantly inside this region, giving large gradient corrections. In the present calculations the use of a pseudopotential results in vanishingly small, but rapidly changing density near the atomic nuclei. The only other region where the PW91 exchange-correlation potential shows large difference from the LDA potential is between the chains of covalent bonds where the electronic density is again very small.

IV. SUMMARY

From the results discussed above, we see that for finite systems (in our study atoms) the PW91 functional improves the LDA results for all the cases we have considered, even though in some cases it overcorrects. When applied to extended systems like solids, the lattice static properties predicted by the PW91 calculation seem to be severely overcorrected, except in simple metals such as Na and Mg. In those situations where PW91 gives an overcorrection, the difference between experiment and theory becomes even larger than in LDA. PW91 does improve the calculated cohesive energies in general. Consequently, it appears that the use of PW91 will be more appropriate in calculations for finite systems[6] or the solids of simple metals.

It is worthwhile to address the question of why the PW91 functional gives such different results when applied to various systems and their physical properties. Apparently, the systems we studied fall into two categories as far as the effect of PW91 is concerned: simple metals, for which a definite improvement over LDA is obtained, and other materials, for which the PW91 results are actually in poorer agreement with experiment than the LDA results. The improvement for the simple metals Na and Mg can be attributed to better description of the exchange-correlation effects between valence and core electrons in a system with smooth electron density and no energy gaps in the quasiparticle spectrum (the reason why PW91 does not give a better description for Al is probably related to the presence of both *s* and *p* valence electrons leading to significant density variations and more covalent bonding). This improvement does not carry over to systems with energy gaps in the quasiparticle spectrum and uneven electronic density distribution, such as the three semiconductors and the insulator examined here. The difficulties of capturing the essential features of the exchange-correlation functional are well known, and are indeed expected to be more severe for cases with gaps in the energy spectrum. Rasolt[25] has recently given a comprehensive discussion of this issue. PW91 does give an improvement for the calculated cohesive energy for all materials we have examined. We suspect that this is due to a better description for the pseudoatom properties in analogy with the improvement in all-electron atomic calculations (see Sec. II).

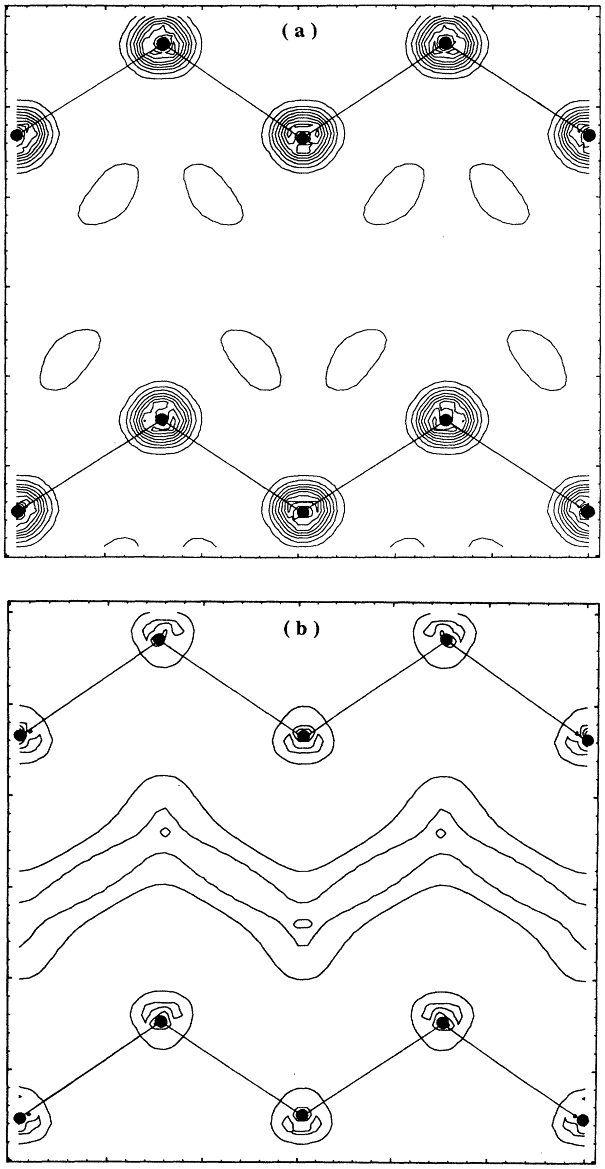

FIG. 4. (a) Difference between PW91 and LDA exchange-correlation energy functionals for Si on the [110] plane of the diamond lattice. Dark symbols indicate the atomic positions. (b) Same as in (a), for the exchange-correlation potentials.

Finally, we compare our results to other recent calculations of similar nature. In Ref. 9 extensive computations have been performed for 3*d*, 4*d*, and 5*d* transition metals using PW91. A general tendency toward increased lattice constants was observed, even though the physical properties of systems considered in Ref. 9 are quite different from the ones considered here. In Ref. 6 solid Na was examined. The difference between the results in Ref. 6 and the present work is small, and can be attributed to the different methodologies. In Ref. 6 the calculation is done with the linear-augmented-plane-wave (LAPW) method, while the pseudopotential approach is adopted in the present work. As far as computational convergence is concerned, consideration of all relevant parameters (such as number of special *k*-points, etc.) leads us to conclude that the results of the present work are as well converged as those of Ref. 6. In Ref. 7 Si, Ge, and GaAs were considered. In Ref. 8 these semiconductors plus Al, Nb, and Pd were examined. There are significant differences between those results and the present work. For example, the lattice constant for Ge is predicted to be 5.71 Å in Ref. 7, 5.62 Å in Ref. 8, and 5.92 Å in the present work. However, different gradient-corrected functionals were employed in the three calculations. In Ref. 7, the semiempirical exchange correction by Becke[26] and the correlation correction by Perdew[27] (BP) were used. In Ref. 8 both BP and an earlier version of the Perdew and Wang functional[11,27] (PW86) were used. It should also be noted that in Ref. 8, the pseudocores from LDA are used for Ge and GaAs, which is in principle inconsistent, although in practice a reasonable approximation. The results of Ref. 8 indicate that PW86 overcorrects LDA more seriously than BP. Moreover, for the calculations of Si, Al, Nb, and Pd in Ref. 8, pseudocores from both LDA and gradient-corrected functionals are used.

It can be seen from those results that the use of pseudocores from gradient-corrected functionals predicts larger lattice constants in some cases. Therefore, all other reported calculations are compatible with the present work after differences in approaches and choices of functionals have been taken into account. In conclusion, we would like to emphasize that all the results presented in this paper were obtained using the specific gradient correction PW91. By comparing to other reported results, it appears that some earlier gradient-corrected functionals, though more empirical, were more successful in predicting the cohesive properties for certain condensed systems than PW91.[7] In view of the considerable differences in the results when different functionals are employed, we conclude that the proper gradient-corrected functional, if one exists, remains elusive.

ACKNOWLEDGMENTS

This work was supported by the Materials Research Laboratory of Harvard University which is funded by National Science Foundation Grant No. DMR 89-20490. The calculations were carried out at the Cornell National Supercomputer Facility. We have benefited from helpful discussions with Dr. M. Rasolt.

APPENDIX A

The PW91 exchange energy functional used in the present calculation is

$$E_x[n] = A_x \int d^3r\, F_x(s) n^{4/3} , \tag{A1}$$

where $n = n(\mathbf{r})$ is the electron density, k_F is the Fermi momentum which is related to the density by $k_F = (3\pi^2 n)^{\frac{1}{3}}$, $A_x = -\frac{3}{4}(\frac{3}{\pi})^{1/3}$, $s = \frac{|\nabla n|}{2k_F n}$, and

$$F_x(s) = \frac{1 + b_1 s y(s) + (b_2 + b_3 e^{-100s^2}) s^2}{1 + b_1 s y(s) + b_4 s^4} ,$$

$$y(s) = \ln[b_5 s + \sqrt{1 + (b_5 s)^2}] .$$

The numerical values of the constants are $b_1 = 0.196\,45$, $b_2 = 0.274\,30$, $b_3 = -0.150\,84$, $b_4 = 0.004$, $b_5 = 7.7956$.

The correlation energy functional is

$$\int d^3r [\epsilon_c(n) + H(n,s,t)] n , \tag{A2}$$

where

$$H = \frac{\beta^2}{(2\alpha)} \ln \left[1 + 2\frac{\alpha}{\beta} \left(\frac{t^2 + At^4}{1 + At^2 + A^2t^4} \right) \right] + C_{c0}[C_c(n) - C_{c1}] t^2 e^{-100s^2} ,$$

$$A = 2\frac{\alpha}{\beta} \left(\frac{1}{e^{-2\alpha\epsilon_c(n)/(\beta^2)} - 1} \right) ,$$

$$C_c(n) = C_1 + \frac{C_2 + C_3 r_s + C_4 r_s^2}{1 + C_5 r_s + C_6 r_s^2 + C_7 r_s^3} ,$$

$$\epsilon_c(n) = -a(1 + \alpha_1 r_s) \ln \left(1 + \frac{1}{a(\beta_1 r_s^{1/2} + \beta_2 r_s + \beta_3 r_s^{3/2} + \beta_4 r_s^{1+p})} \right) .$$

The density dependent variables t, k_s, and r_s are defined as $t = \frac{|\nabla n|}{(2k_s n)}$, $k_s = (\frac{4k_F}{\pi})^{1/2}$, $r_s = (\frac{3}{4\pi n})^{1/3}$, and the numerical values of the constants are $\alpha = 0.09$, $\beta = 0.066\,726\,321\,2$, $C_{c0} = 15.755\,92$, $C_{c1} = 0.003\,521$, $C_1 = 0.001\,667$, $C_2 = 0.002\,568$, $C_3 = 0.023\,266$, $C_4 = 7.389 \times 10^{-6}$, $C_5 = 8.723$, $C_6 = 0.472$, $C_7 = 7.389 \times 10^{-2}$, $a = 0.062\,181\,4$, $\alpha_1 = 0.213\,70$, $\beta_1 = 7.5957$, $\beta_2 = 3.5876$, $\beta_3 = 1.6382$, $\beta_4 = 0.492\,94$, $p = 1.00$. All values are in atomic units.

APPENDIX B

It is convenient to use the BHS pseudopotentials as a starting point to build the new gradient-corrected pseudopotentials. This results in substantial savings of computational effort without any loss of flexibility. Moreover, the widely used BHS pseudopotentials can be simply modified to obtain the gradient-corrected potentials. The basic idea is as follows: consider a valence state of angular momentum l. The Schrödinger equation for the radial part of the wave function is

$$\left[-\frac{1}{2m}\frac{d^2}{dr^2} + \frac{l(l+1)}{2mr^2} + V(r) \right] \phi_l(r) = \epsilon_l \phi_l(r) \tag{B1}$$

(in atomic units, with $\hbar = 1$). Both $\phi_l(r)$ and the DFT potential (including gradient corrections) $V(r)$ can be obtained from a self-consistent all-electron calculation. The pseudopotential equation is

$$\left[-\frac{1}{2m}\frac{d^2}{dr^2}+\frac{l(l+1)}{2mr^2}+V_{\mathrm{ps}}(r)\right]\tilde{\phi}_l(r)=\epsilon_l\tilde{\phi}_l(r)\ , \quad \text{(B2)}$$

where $V_{\mathrm{ps}}(r)$ is the screened pseudopotential which includes the gradient corrections, and outside a cutoff radius r_c , $\tilde{\phi}_l(r)=\phi_l(r)$. The Schrödinger equation corresponding to the BHS pseudopotential is

$$\left[-\frac{1}{2m}\frac{d^2}{dr^2}+\frac{l(l+1)}{2mr^2}+V_{\mathrm{ps}}^{\mathrm{BHS}}(r)\right]\tilde{\phi}_l^{\mathrm{BHS}}(r) = \epsilon_l^{\mathrm{BHS}}\tilde{\phi}_l^{\mathrm{BHS}}(r)\ . \quad \text{(B3)}$$

We define $\Delta\tilde{\phi}_l(r)=\tilde{\phi}_l(r)-\tilde{\phi}_l^{\mathrm{BHS}}(r)$. Outside the cutoff radius, $\Delta\tilde{\phi}_l(r)$ is known exactly, since both $\tilde{\phi}_l(r)$ and $\tilde{\phi}_l^{\mathrm{BHS}}(r)$ can be obtained from a self-consistent calculation. Notice that outside the core $\tilde{\phi}_l(r)=\phi_l(r)$. However, since these two wave functions belong to potentials that include gradient corrections, they are different from $\tilde{\phi}_l^{\mathrm{BHS}}(r)$. For $r<r_c$, we expand $\Delta\tilde{\phi}_l(r)=\sum_{n=0}^{3}c_n r^{l+2n}$. By requiring that $\tilde{\phi}_l(r)$ and its first and second derivatives are continuous at r_c, and imposing the normalization condition, we can solve for the coefficients c_n, $n=0,\ldots,3$. In order to satisfy Eq. (B2), $\Delta V_{\mathrm{ps}}(r)=V_{\mathrm{ps}}(r)-V_{\mathrm{ps}}^{\mathrm{BHS}}(r)$ must satisfy

$$\Delta V_{\mathrm{ps}}(r)=\epsilon_l-\frac{\epsilon_l^{\mathrm{BHS}}\tilde{\phi}_l^{\mathrm{BHS}}(r)}{\tilde{\phi}_l^{\mathrm{BHS}}(r)+\Delta\tilde{\phi}_l(r)}-\frac{\tilde{f}(r)}{\tilde{\phi}_l^{\mathrm{BHS}}(r)+\Delta\tilde{\phi}_l(r)}\ , \quad \text{(B4)}$$

where

$$\tilde{f}(r)=\left[-\frac{1}{2m}\frac{d^2}{dr^2}+\frac{l(l+1)}{2mr^2}+V_{\mathrm{ps}}^{\mathrm{BHS}}\right]\Delta\tilde{\phi}_l(r). \quad \text{(B5)}$$

Since $\Delta\tilde{\phi}_l(r)$ is exactly known everywhere, we can use Eq. (B4) to obtain the screened pseudopotential $V_{\mathrm{ps}}(r)$. By calculating the PW91 exchange-correlation potential and the Hartree potential from the density corresponding to the pseudo wave function $\tilde{\phi}_l(r)$, we unscreen the pseudopotential and get the bare pseudopotential $V_{\mathrm{ps}}^{\mathrm{ion}}(r)$ to be used in the solid calculation. We then fit the numerical result for the new pseudopotential to the same functional form as in the BHS pseudopotential. For simplicity, we only refit the coefficients of the short range l-dependent part. This procedure offers the important advantage of avoiding highly nonlinear fits. In Fig. 5 we compare the new pseudopotential and the BHS pseudopotential for Si. As is seen from this figure, the new pseudopotential is comparable to the BHS pseudopotential in terms of well depth and curvature.

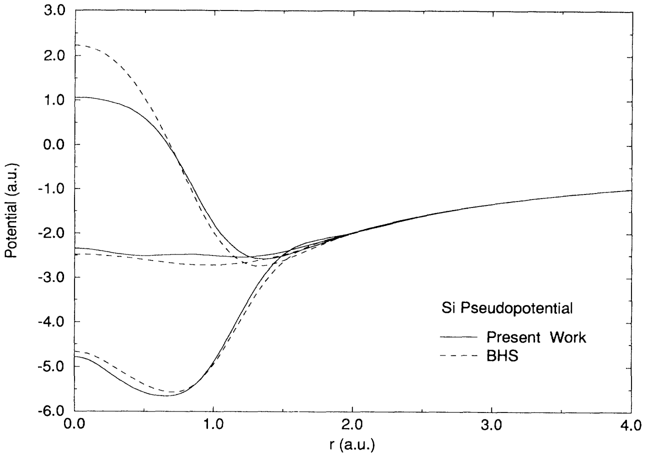

FIG. 5. The new (gradient-corrected) and BHS pseudopotential for Si.

Here we should like to point out that the PW91 exchange-correlation potential corresponding to the pseudo wave function exhibits pathological behavior near the origin (oscillations of increasing amplitude), which makes the creation of a smooth pseudopotential impossible. For this reason, we introduce a cutoff function $1/(1+e^{(r_{c0}-r)/\delta})$, where r_{c0} and δ are adjustable parameters and are both much smaller than the cutoff radius r_c. By multiplying the PW91 exchange-correlation potential with this cutoff function, we make the potential go smoothly to zero near the origin, which makes the creation of a well behaved pseudopotential possible. This procedure is justified on grounds that the properties of the solid should not depend on features of the pseudopotential inside the core. Similar problems with the behavior of gradient corrections near the origin were noticed by Ortiz and Ballone.[4]

---

[1] P. Hohenberg and W. Kohn, Phys. Rev. **136**, B864 (1964).

[2] W. Kohn and L. Sham, Phys. Rev. **140**, A1133 (1965).

[3] For a recent review of this methodology see R.O. Jones and O. Gunnarson, Rev. Mod. Phys. **61**, 689 (1984).

[4] G. Ortiz and P. Ballone, Phys. Rev. B **43**, 6376 (1991).

[5] P. Bagno, O. Jepsen, and O. Gunnarsson, Phys. Rev. B **40**, 1997 (1989).

[6] J.P. Perdew, J.A. Chevary, S.H. Vosko, K.A. Jackson, M.R. Pederson, D.J. Singh, and C. Fiolhais, Phys. Rev. B **46**, 6671 (1992).

[7] G. Ortiz, Phys. Rev. B **45**, 11 328 (1992).

[8] A. Garcia, C. Elässer, J. Zhu, S.G. Louie, and M. Cohen, Phys. Rev. B **46**, 9829 (1992).

[9] M. Körling and J. Häglund, Phys. Rev. B **45**, 13 293 (1992).

[10] J.P. Perdew, in *Electronic Structure of Solids '91*, edited by P. Ziesche and H. Eschrig (Akademie Verlag, Berlin, 1991).

[11] J.P. Perdew and Y. Wang, Phys. Rev. B **33**, 8800 (1986).

[12] D. Liberman, J.T. Waber, and D.T. Cromer, Phys. Rev. **137**, A27 (1965).

[13] M.T. Carroll, R.F.W. Bader, and S.H. Vosko, J. Phys. B **20**, 3599 (1987).

[14] R.G. Parr and W. Yang, *Density-Functional Theory of Atoms and Molecules* (Oxford University Press, Oxford, 1989).

[15] D.M. Ceperley and B.J. Alder, Phys. Rev. Lett. **45**, 566 (1980); J. Perdew and A. Zunger, Phys. Rev. B **23**, 5048

(1981).

[16] G.B. Bachelet, D.R. Hamann, and M. Schlüter, Phys. Rev. B **26**, 4199 (1982).

[17] F.D. Murnaghan, Proc. Natl. Acad. Sci. U.S.A. **30**, 244 (1944).

[18] N.W. Ashcroft and N.D. Mermin, *Solid State Physics* (Rinehart and Winston, New York, 1975).

[19] M.L. Cohen and J.R. Chelikowsky, *Electronic Structure and Optical Properties of Semiconductors* (Springer, New York, 1988).

[20] C. Kittel, *Introduction to Solid State Physics,* 4th ed. (Wiley, New York, 1971).

[21] G. Simmons and H. Wang, *Single Crystal Elastic Constants and Calculated Aggregate Properties: A Handbook,* 2nd ed. (MIT Press, Cambridge, 1971).

[22] W.A. Harrison, *Electronic Structure and the Properties of Solids* (Freeman, San Francisco, 1980).

[23] O. Madelung, *Semiconductors of Group IV Elements and III-V Compounds* (Springer, New York, 1991).

[24] U. Rössler and O. Schütz, Phys. Status Solidi B **56**, 296 (1973).

[25] M. Rasolt, in *Handbook on Semiconductors*, edited by P.T. Landsberg (North-Holland, Amsterdam, in press).

[26] A.D. Becke, Phys. Rev. A **38**, 3098 (1988).

[27] J.P. Perdew, Phys. Rev. B **33**, 8822 (1986).